STRUCTURE OF THE MARINE ATMOSPHERIC BOUNDARY LAYER DURING TWO COLD AIR OUTBREAKS OF VARYING INTENSITIES: GALE 86

ROBERT J. WAYLAND* and SETHU RAMAN

North Carolina State University, Department of Marine, Earth and Atmospheric Sciences, Raleigh, North Carolina 27695, USA

(Received in final form 11 March, 1994)

Abstract. Aircraft, surface, upper air and satellite measurements have been used to observe the evolution and growth of the convective Marine Atmospheric Boundary Layer (MABL) offshore of North Carolina in close proximity to the Gulf Stream, during the intense cold air outbreak of 28 January 1986 and the moderate event of 12 February 1986, as part of the Genesis of Atlantic Lows Experiment (GALE). Air mass modification processes, driven primarily by the ocean-atmosphere exchanges of surface turbulent sensible and latent heat fluxes, caused the overlying air mass to warm and moisten as it advected over the warmer waters of the eastern United States continental shelf. Maximum observed near-surface total heat fluxes were 1045 and 811 $W \cdot m^{-2}$ over the core of the Gulf Stream, for 28 January and 12 February 1986, respectively. The observed changes in the overlying air mass occurred almost instantaneously as the ambient flow traversed different underlying SST conditions.

The turbulent structure showed a buoyancy-dominated MABL below approximately $0.8z/h$. However, shear was also observed to be an important production term above $0.8z/h$ and below $0.1z/h$ for the 28 January 1986 event. Dissipation of turbulent kinetic energy was the dominant destruction term in the budgets, but vertical transport of energy was a strong contributor below $0.5z/h$, above which this term became a source of turbulent energy. Additionally, the normalized standard deviations of the horizontal velocity components showed a near-equal contribution to the turbulence, while the vertical velocity components displayed the characteristic mid-layer maximum profile observed for a convective, well-mixed boundary layer.

1. Introduction

Latent and sensible heat exchanges between the ocean-atmosphere systems have long been investigated during cold air outbreaks (Kondo, 1976; Lenschow and Agee, 1976; Lenschow *et al.*, 1980; Chou and Atlas, 1982; Chou *et al.*, 1986; SethuRaman *et al.*, 1986; Bane and Osgood, 1989; Brümmer *et al.*, 1992). The geographic conditions are optimized along eastern continental margins during the winter months (November–March) for these events. The unique geographic conditions arise due to the presence of a strong, relatively warm western boundary current (e.g., Kuroshio and Gulf Stream systems) flowing in close proximity to the coastal margins, which create very strong cross-shelf thermal gradients. These gradients cause rapid transformations in overlying air masses as they traverse this

* Current affiliation: Science Application Int. Corp., Technology Assessment Div., 615 Oberlin Rd., Raleigh, NC, 27605, USA.

Boundary-Layer Meteorology **71**: 43–66, 1994.

region, generating a strongly baroclinic Marine Atmospheric Boundary Layer (MABL).

Cold air outbreaks (CAOs) occur when a cold, dry continental air mass of Polar origin advances out over the warmer oceanic region. Recent investigations along the eastern United States coast have shown that 15–20 CAOs occur annually, with approximately five of these events being classified as severe or extreme (e.g., air temperature $< 0\,^{\circ}C$ and core Gulf Stream temperature $\geq 20\,^{\circ}C$). Generally, each event has a duration or maximum impact on the region on the order of 24 to 48 h (Grossman, 1988; Konrad and Colucci, 1989; Grossman and Betts, 1990). For the Gulf of Mexico region, CAOs have been observed to occur at 3–10 day intervals from October to April and their impacts have been shown to be highly dependent on the air-sea surface temperature (SST) gradient, vertical humidity structure and the wind speed (Fernandez-Partegas, 1975; Huh *et al.*, 1984). Each of these parameters has been observed to change rapidly across the inner continental shelf of the mid-Atlantic coastal region during CAO conditions (Chou and Atlas, 1982; Wayland and Raman, 1989; Wayland, 1991).

The objectives of this research are to compare and contrast both the mean and turbulent MABL structure for two CAO events of varying intensities, which occurred during the Genesis of Atlantic Lows Experiment (GALE-86). GALE was conducted in the mid-Atlantic coastal region of the United States, centered along the area offshore of North Carolina between 15 January 1986 and 15 March 1986. The project utilized aircraft, radar, sounding, satellite and surface-based observations to monitor both the synoptic and mesoscale changes in atmospheric/oceanic conditions. A detailed account of the overall program is found in Dirks *et al.* (1988), while a complete description of the Planetary Boundary Layer (PBL) sub-program is given by Raman and Riordan (1988). This study focuses on the strong, intense cold air outbreak of 28 January 1986 (air-SST $\sim 25\,^{\circ}C$) and the milder event on 12 February 1986 (air-SST $\sim 19\,^{\circ}C$).

2. Observations

2.1. Introduction

The initial flight and cruise plans for each Intensive Observation Period (IOP) discussed below were designed to allow a reasonable and accurate reconstruction of the mean and turbulent structure of the MABL offshore of the Wilmington and Cape Hatteras, North Carolina areas. However, due to in-flight logistics changes, these objectives were not always accomplished and suitable alternate plans were implemented to minimize their impact on research operations.

For each of the two CAO events investigated, a multi-faceted data set was available. The foundation for each investigation was comprised of measurements from the NCAR Electra and King Air aircraft missions, R6, R8, R14, R15 and R16, which supplied the bulk of the information utilized. However, a great contri-

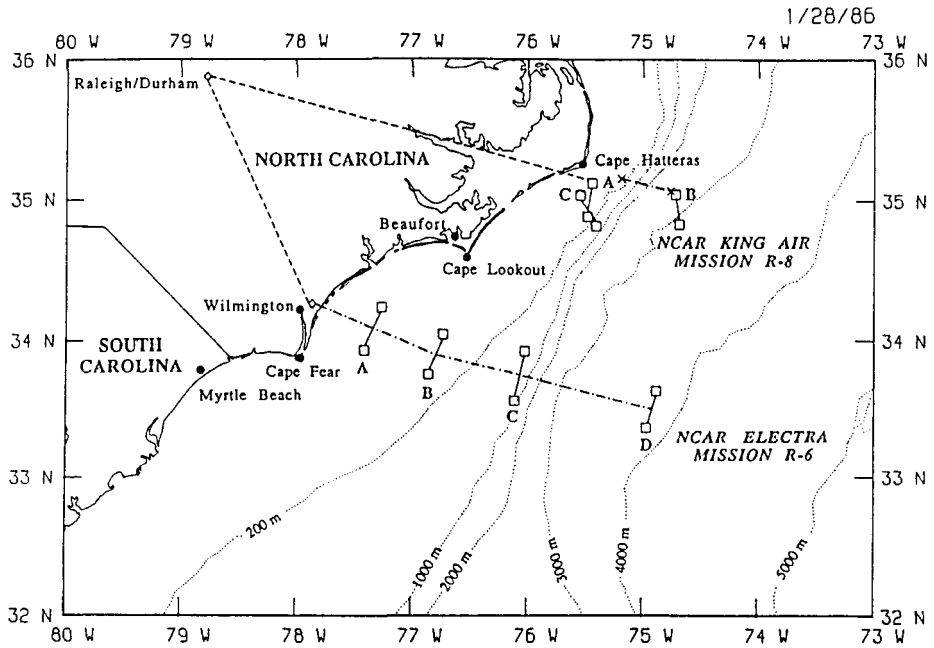

Fig. 1. Map detailing the flight plan and geographic locations for the research stations occupied during the 28 January 1986 NCAR Electra and King Air Missions (R-6 and R-8, respectively).

bution to the overall synthesis effort was made through the various ancillary data sets which were analyzed. These data sets consisted of the Portable Automated Mesonet-II (PAM-II) data, the surface marine network, consisting of National Data Buoy Center (NDBC) buoys and the Coastal-Marine Automated Network (C-MAN) stations, the North Carolina State University (NCSU) buoy network and the Ships-of-Opportunity (SOOP), the upper atmospheric sounding network and the oceanographic support provided by the R/V CAPE HATTERAS and the National Oceanographic and Atmospheric Administration (NOAA) Polar Orbiting Satellite systems (NOAA-7 and 9). See Wayland (1991) for more details.

2.2. 28 January 1986 strong CAO

The 28 January 1986 research missions were conducted as part of Intensive Observation Period (IOP) 2, which included four major events: (1) Cold Air Damming; (2) Coastal Frontogenesis; (3) Offshore Cyclogenesis; and, (4) Cold Air Cyclogenesis (Mercer and Kreitzberg, 1986). IOP 2 is best remembered for the extremely intense cold air outbreak of 28 January 1986, which coincided with the tragic mechanical failure and explosion of the Space Shuttle Challenger. Figure 1 is a map outlining the flight plan and geographic locations of the research stations for the NCAR Electra and King Air missions (R-6 and R-8, respectively).

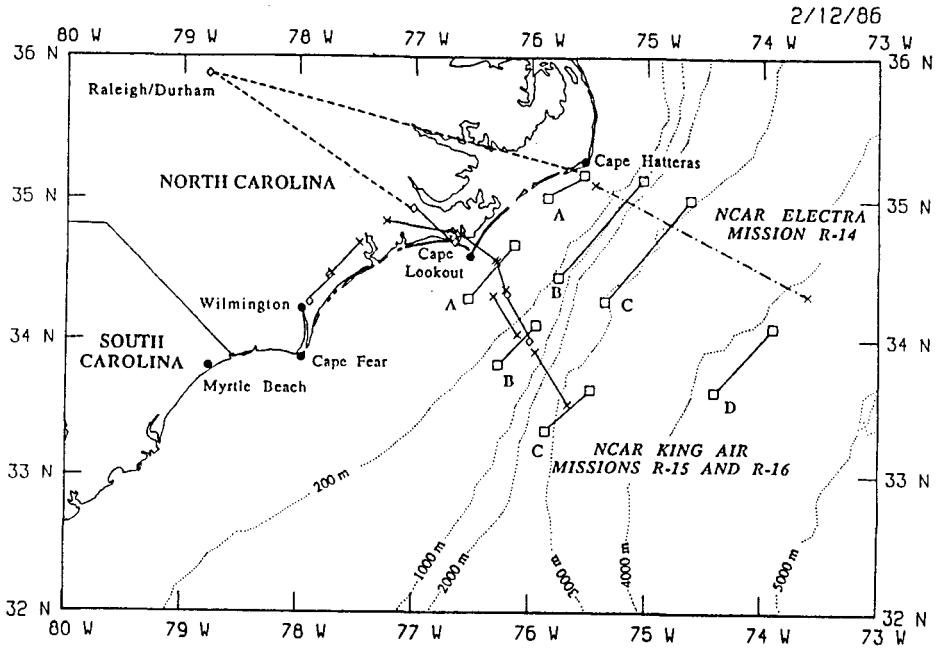

Fig. 2. Map detailing the flight plan and geographic locations for the research stations occupied during the 12 February 1986 NCAR Electra and King Air Missions (R-14 and R-15/16, respectively).

2.3. 12 February 1986 moderate CAO

The 12 February 1986 research missions were conducted as part of IOP 5: (1) Offshore Cyclogenesis; and, (2) CAO. This particular CAO event was relatively mild in comparison to the 28 January 1986 event and provided a unique opportunity to compare the similarities/differences in MABL structure between an intense and a moderate cold air outbreak. Figure 2 details the flight track and research stations for NCAR Electra and King Air missions (R-14 and R-15/16, respectively).

3. Synoptic Conditions

3.1. 28 January 1986 strong CAO

A detailed analysis of the synoptic conditions on 28 January 1986, as related to the Challenger disaster, is given by Uccellini *et al.* (1986). Figure 3 presents six-hourly summary synoptic charts for the surface meteorological conditions on 28 January 1986. The synoptic maps demonstrate an intense CAO episode in the GALE region, which was associated with two developing surface systems. First, a strong developing high pressure ridge along the Texas Gulf Coast was broadening and beginning to move towards the eastern seaboard of the United States. Additionally, this anticyclone was working in tandem with a rapidly intensifying

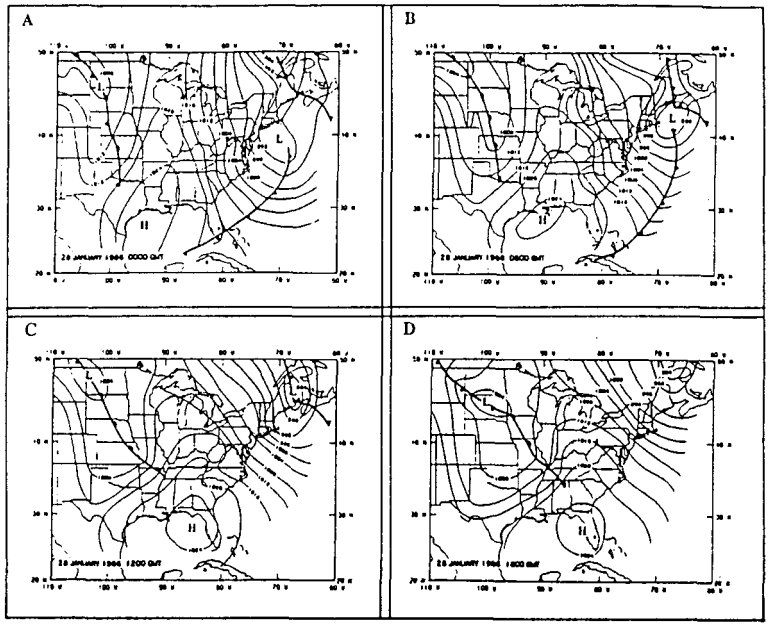

Fig. 3. Summary surface synoptic weather charts for 28 January 1986: (a) 0000 GMT; (b) 0600 GMT; (c) 1200 GMT; and, (d) 1800 GMT.

extratropical cyclone which was moving out of the GALE research area towards the northeast. The combined circulations (e.g., anticyclonic and cyclonic, respectively) of the two systems served to channel the dry, cold Continental Polar air mass into the GALE research area.

The PAM-II Network stations showed sub-freezing air temperatures throughout North and South Carolina, while when combined with the Surface Marine Layer Data, the surface freezing isopleth was evident near the shelf break at 0000 GMT. During the afternoon hours, the surface freezing isopleth extended as far offshore as the western wall of the Gulf, Stream, prior to retreating shoreward late in day. The surface wind field showed a predominantly W to NW flow throughout the GALE study area, which tended to accelerate over the ocean region. However, winds decreased throughout the day, primarily in response to the weakening pressure gradient. Additionally, the 0000 GMT coastal soundings at Cape Hatteras (HAT) and Morehead City (MRH) showed a strong backing of the wind with height which is indicative of cold air advection.

3.2. 12 February 1986 moderate CAO

The 12 February 1986 moderate CAO event was contained within IOP 5 and followed the investigation of an onshore-flow/coastal front event, two days earlier. In contrast to the conditions present on 28 January 1986, the pressure gradient between the deepening offshore cyclone and the building midwestern anticyclone

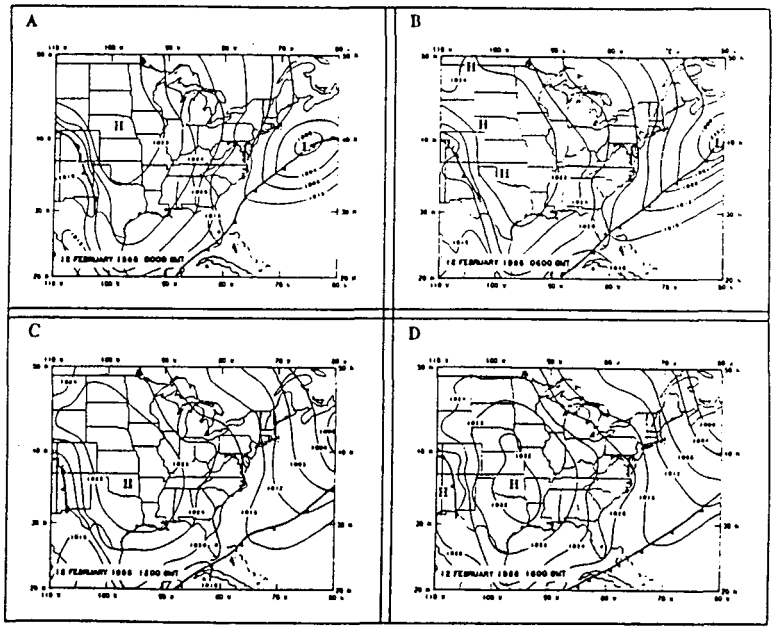

Fig. 4. Summary synoptic surface weather charts for 12 February 1986: (a) 0000 GMT; (b) 0600 GMT; (c) 1200 GMT (d) 1800 GMT.

was not very strong and the infiltrating air mass, while of Canadian origin, was not as bitterly cold as its counterpart on 28 January 1986. Figure 4 presents the six-hourly summary synoptic surface meteorological charts for conditions within the study area on 12 February 1986. However, in analyzing this CAO it is beneficial to examine the surface air temperature and wind fields six hours prior to the onset of the CAO (e.g., 11 February 1986 1800 GMT) to show the strong influence of the decaying frontal zone on the region.

The PAM-II Network data for 11 February 1986 1800 GMT, showed that the entire GALE region (minus the extreme northwestern Appalachians) had air temperatures above the freezing level. Moving offshore, the above-freezing air temperatures continued, establishing a strong NW to SE gradient across the study area. The surface wind field analyses showed that the flow was predominantly from the NW over much of North Carolina, but turned more WSW over South Carolina. The remnant frontal feature was easily detected in the Marine Surface Layer analysis by a distinct wind shift line. Thus, the oncoming cold air mass would have to displace this much warmer wedge of air over the southeastern study area, causing some air mass modification to occur prior to its reaching the offshore waters of the Gulf Stream and the Sargasso Sea.

The 0000 GMT surface air temperatures revealed the initial movement of the cold, dry air into the region from the north, which is seen in the sub-zero temperatures along the Virginia-North Carolina border. The surface winds were predomin-

antly NNW over the majority of the region, except for the extreme southern and offshore areas where westerly winds prevailed. Additionally, 0000 GMT soundings from Cape Hatteras (HAT) and Wilmington (ILM) exhibited strong backing of the wind (e.g., cold air advection) within the lowest 1500 m of the atmosphere, which was also observed for the 28 January 1986 investigation. As the day progressed, the cyclone continued to move away from the study area, reducing its influence, while the ridging anticylcone continued to increase in areal extent and migrate towards the southeastern United States.

Thus, the combined circulations of the building anticyclone and the departing offshore cyclone continued to funnel cold air into the research area, very similar to the processes operating on 28 January 1986. However, during the current cold air outbreak, neither the pressure gradient between the two systems nor the low temperatures of the ensuing air mass were as prominent as in the earlier event. These factors combined to provide the moderate cold air outbreak of 12 February 1986, which was much less spectacular than the one on 28 January 1986. The more northerly trajectory of the air flow allowed a degree of air mass modification to occur prior to the air parcels reaching the waters offshore of Cape Hatteras, North Carolina. This strongly contrasts with the 28 January 1986 event in which the air mass approached the coastal zone predominantly from the west, providing little chance for upwind air mass modification to occur due to interaction with warmer underlying oceanic surfaces.

4. Discussion of Results

4.1. Mean MABL structure

Vertical variation of the mean values of wind speed, wind direction, potential temperature (θ) and specific humidity (q) at different locations across the North Carolina shelf (offshore of Wilmington) for NCAR Electra Mission R-6 are shown in Figure 5. In general, the cloud layer deepened in the downwind direction beginning at Station B in response to increasing thermal contrast and turbulence. These changes were observed in a rapidly decreasing cloud base and increasing MABL height along the flight trajectory. The details of the mean and turbulent structure for the 28 January 1986 Electra Mission R-6 can be found in Wayland and Raman (1989) and Wayland (1991).

The vertical variation of the mean values of wind direction and speed, potential temperature (θ) and specific humidity (q) at the three research stations located just offshore of Cape Hatteras for NCAR King Air Mission R-8 are presented in Figure 6. Cloud base decreased slightly in the offshore direction for this mission, but not as dramatically as during the NCAR Electra mission (R-6). This reduction in cloud base coupled with the growth of the cloud tops in the offshore direction again created a cloud layer which was expanding in depth in the offshore direction.

At Stations A and B, the wind direction was observed to back between the

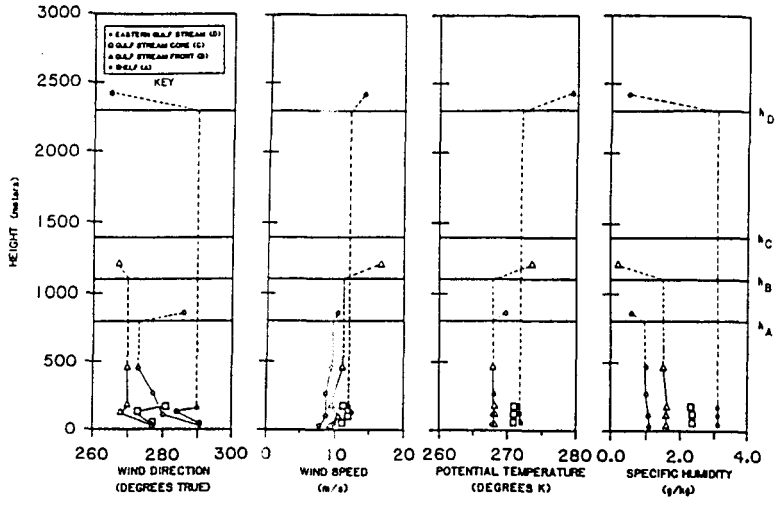

Fig. 5. Mean boundary-layer structure as measured by crosswind profiles of wind direction, wind speed, potential temperature and specific humidity for NCAR Electra Mission R-6 on 28 January 1986. Dashed lines indicate regions where no data were collected.

lowest two levels. However, on the return to the nearshore region (Station C) near the end of the mission (~1900 GMT), the low-level winds did not display this behavior, indicating the end of the strong cold air advection along the inner shelf. These results are also in good agreement with both the NCAR Electra data and the coastal upper air soundings, which showed strong low-level cold air advection early in the day (0000 GMT) which gradually decreased prior to ending near 1800 GMT. Additionally, the wind direction also veered in the offshore direction between the coast and Station B, as was also observed by the NCAR Electra. This initial turning of the wind to the right could again be in response to the decrease in surface roughness as the air flow makes the transition from over the land to over the water.

The low-level (~50 m) wind speed increased with time during NCAR King Air Mission R-8. The maximum observed low-level wind speed was $13.2\,m \cdot s^{-1}$ at Station C. Additionally, as was observed by the NCAR Electra, wind speeds also increased between Stations A ($8.8\,m \cdot s^{-1}$) and B ($10.7\,m \cdot s^{-1}$) across the Gulf Stream Front during the outbound phase of the mission. The low-level jet feature which was observed at each of the four crosswind research stations by the NCAR Electra was only documented at Station A during the current mission. However, the jet observed at Station A extended upward from 100 m to almost 250 m, in contrast to the narrowly defined feature observed by the NCAR Electra offshore of Wilmington.

The potential temperature profiles show the response of the MABL to the strong surface heating over this region. Given the Gulf Stream's close proximity

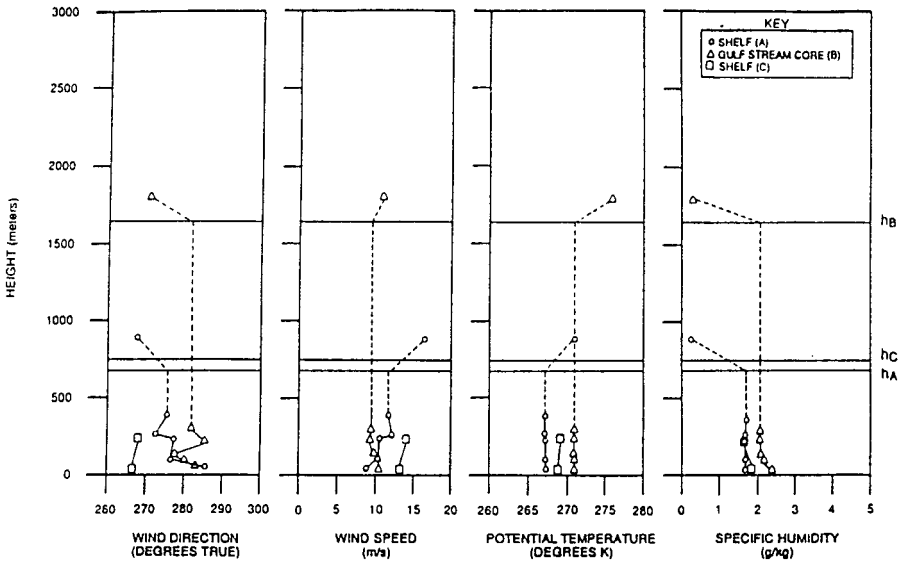

Fig. 6. Mean boundary-layer structure as measured by crosswind profiles of wind direction, wind speed, potential temperature and specific humidity for NCAR King Air Mission R-8 on 12 February 1986. Dashed lines indicate regions where no data were collected.

to Cape Hatteras, the oceanic temperature gradients in this region can be quite large. The minimum and maximum temperatures were measured at Station A (267.4° K) and Station B (271.1° K), respectively. On the return to the shelf area (Station C), the mixed-layer temperature had increased to 269.3° K, showing an increase of 1.9° K in approximately two hours (e.g., $1° K \cdot h^{-1}$). The mean cross-Stream gradient in air temperature for NCAR King Air Mission R-8 was computed to be $0.0569° K \cdot km^{-1}$, which was substantially higher than the gradient observed by the NCAR Electra offshore of Wilmington, North Carolina.

The specific humidity profiles for this mission also showed the characteristics of a well-developed mixed layer where the low-level measurements ranged from $1.72 g \cdot kg^{-1}$ (Station A) over the shelf to $2.37 g \cdot kg^{-1}$ (Station B) over the core of the Gulf Stream. Station C showed a moderate increase in specific humidity ($1.78 g \cdot kg^{-1}$) over the two-hour duration of the aircraft mission. Once again these profiles correlated well with the observed inversion levels in potential temperature. Additionally, the specific humidity gradient across the Stream (between Stations A and B) was $0.0100 g \cdot kg^{-1} \cdot km^{-1}$ which was in good agreement with the NCAR Electra results. Thus, in the area offshore of Cape Hatteras, the rate of change in the overlying air mass was almost five times faster for temperature than for moisture.

The vertical variations of wind direction and speed, potential temperature (θ) and specific humidity for the 12 February 1986 NCAR Electra Mission R-14, which was conducted offshore of Morehead City/Beaufort, North Carolina, are shown

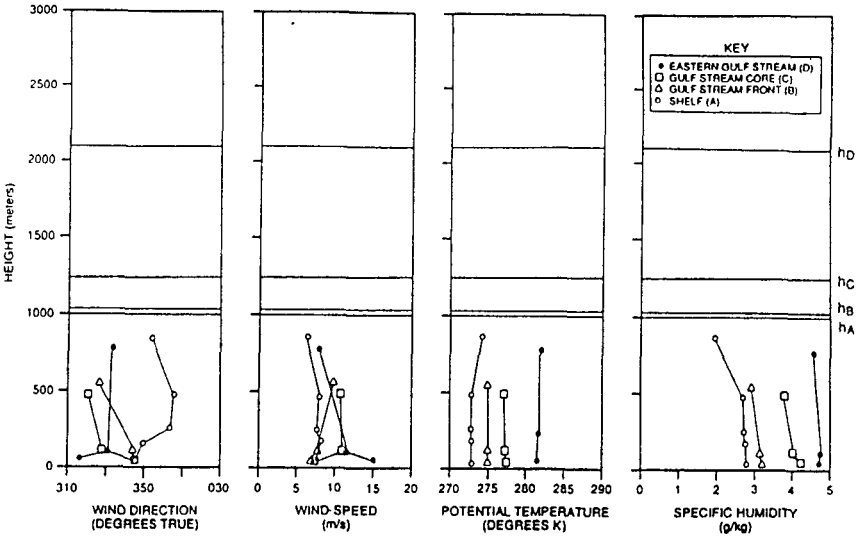

Fig. 7. Mean boundary-layer structure as measured by crosswind profiles of wind direction, wind speed, potential temperature and specific humidity for NCAR Electra Mission R-14 on 12 February 1986.

in Figure 7. In contrast to the 28 January 1986 observations, the inner shelf (Station A) and the Sargasso Sea (Station D) wind profiles were not observed to back with height between the lowest two crosswind flux levels. However, the Gulf Stream Front (Station B) showed moderate backing with height while the Gulf Stream Station C showed strong cold air advection between these two lowest levels. In addition, over the latter two locations the backing of the wind continued up to approximately 500 m. The characteristic turning of the wind to the right over the two nearshore stations, which was observed on 28 January 1986, was not observed here as Stations A, B and C maintained an almost constant low-level wind direction across the shelf. This difference can be attributed to the difference in the mean synoptic flow for the cold air outbreaks being studied. The 28 January 1986 flow was predominantly westerly from over the continent, whereas the 12 February circulation was more northerly and had an over-ocean trajectory for much of the offshore GALE study region. This difference allowed the surface winds for 12 February 1986 to adjust to the changes in roughness prior to reaching the offshore research locations.

The wind speed profiles for the three research stations each exhibited a low-level (~100 m) jet feature and are in good general agreement with the 28 January 1986 aircraft findings. The maximum observed low-level (~50 m) wind speed was 15.1 $m \cdot s^{-1}$ over the Sargasso Sea area (Station D), but over the Stream and inner shelf, the maximum observed values were over one-half this magnitude (Station A = 7.3 $m \cdot s^{-1}$; Station B = 6.9 $m \cdot s^{-1}$; and Station C = 6.8 $m \cdot s^{-1}$). In general,

excluding Station D, the wind speeds were much lower for the 12 February 1986 CAO and the acceleration of the low-level winds toward the Gulf Stream/Gulf Stream Front which were observed on 28 January 1986 were not evident in these data. Again this can possibly be attributed to the more northerly trajectory of the synoptic flow for this event.

The potential temperature profiles, aside from being generally warmer than those for 28 January 1986 also exhibited greater horizontal variation in the cross-shelf direction. Changes in mixed-layer temperatures for 28 January 1986 were on the order 5.9 and 3.7° K for the NCAR Electra and King Air missions, respectively. However, the 12 February 1986 changes in mixed-layer temperature were 8.5° K (Station A = 273.0° K; Station B = 275.0° K; Station C = 277.4° K; and, Station D = 281.5° K). The resulting cross-shelf (Station A to D) air temperature gradient was $0.0445° K \cdot km^{-1}$ with a maximum gradient of $0.0600° K \cdot km^{-1}$ between the Gulf Stream Front (Station B) and the core of the Stream (Station C). These gradients were considerably larger than those computed for the earlier NCAR Electra mission (R-6), but were comparable to those computed for the NCAR King Air mission (R-8), which was operating in this same general geographic area on 28 January 1986. The biggest contrast to the earlier CAO was that all research locations across the region showed low-level air temperatures greater than or equal to the freezing point (~273° K), because the 28 January 1986 aircraft missions experienced sub-freezing low-level temperatures across the shelf and over the Stream.

As was noted above for the air temperature, the air mass over the study area was also much wetter during the 12 February 1986 investigation than during the previous CAO. However, the specific humidity profiles continued to show the characteristics of a well-mixed convective boundary layer and supported the inversion levels observed in the potential temperature profiles. The low-level specific humidity values ranged from $2.80 g \cdot kg^{-1}$ over the shelf (Station A) to $4.69 g \cdot kg^{-1}$ in the Sargasso Sea area (Station D). At Stations B and C, observed low-level data values were 3.20 and $4.19 g \cdot kg^{-1}$, respectively. The cross-shelf moisture gradient ($0.0099 g \cdot kg^{-1} \cdot km^{-1}$) between Stations A and D was comparable to the earlier aircraft results from 28 January 1986. Thus, the MABL offshore of Morehead City/Beaufort, North Carolina on 12 February 1986 was warmer and wetter than the 28 January 1986 scenario, but in general showed lower wind speeds across the inner and outer shelf areas.

The vertical variation of the wind direction and speed, potential temperature (θ) and specific humidity for NCAR King Air Missions R-15 and R-16 are presented together in Figure 8 since the latter mission was merely a continuation of the earlier mission and is synoptic in terms of temporal and spatial coverage. The wind direction profiles show a difference between the inshore, mid-shelf location (Station A) and the remaining two offshore stations (Stations B and C). The offshore locations exhibit the characteristic backing of the wind with height between the first two levels, while the mid-shelf location (Station A) shows strong

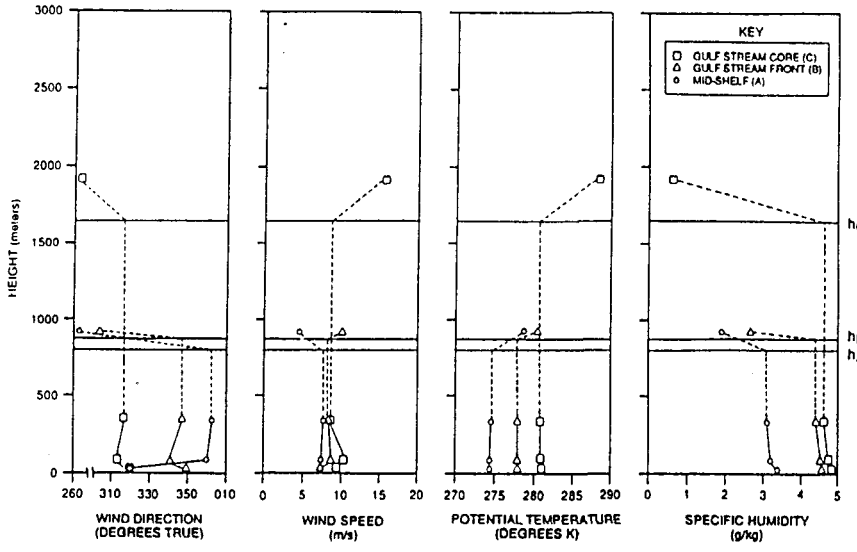

Fig. 8. Mean boundary-layer structure as measured by crosswind profiles of wind direction, wind speed, potential temperature and specific humidity for NCAR King Air Missions R-15/16 on 12 February 1986. Dashed lines indicate regions where no data were collected.

low-level veering with height. The probable explanation for this observation is that the more northerly flow observed on 12 February 1986 causes the air to approach Stations B and C from over the open ocean, allowing the near-surface wind direction to adjust to the changes in surface roughness (z_0), which can be approximately two to three orders in magnitude between land and the open ocean. However, Station A is close to the coast and shows this adjustment, where the near-surface wind direction is observed to turn to the right in response to reduced surface roughness, increasing wind speed and the resultant increased influence of the Coriolis parameter. The combination of these three factors causes the wind to veer at the lower levels at Station A as opposed to the results observed farther offshore where the air mass has had sufficient time to adjust.

The effect of the possible wind shadow is also seen in the wind speed profiles, where the Gulf Stream Front (Station B) and the Gulf Stream (Station C) locations showed the low-level (~90 m) jet feature, while the nearshore location (Station A) showed only a relatively constant vertical wind profile (~7.5 m · s^{-1}). In contrast to the 12 February 1986 NCAR Electra mission (R-14) and in relative agreement with the 28 January aircraft results, the wind speed increased in the offshore direction, accelerating towards the Gulf Stream. Maximum observed low-level (~40 m) wind speed was 9.6 m · s^{-1} over the core of the Stream (Station C). Landward of this location, wind speed decreased to 7.7 m · s^{-1} at the Gulf Stream Front (Station B) and to 7.6 m · s^{-1} at the shelf location (Station A). Thus, in general these wind speeds were greater than those measured by the NCAR Electra,

which was operating to the north of this region, but were less than those observed by either aircraft during the 28 January 1986 CAO.

The potential temperature profiles for this mission show the characteristic strong capping inversion with a well-mixed boundary layer underneath. Mixed-layer temperatures ranged from 274.5° K at the mid-shelf location (Station A) to 278.1° K along the Gulf Stream Front (Station B) before reaching the maximum observed low-level value of 280.9° K over the core of the Stream. As was observed in the NCAR Electra observations for this date, all crosswind research stations observed low-level air temperatures greater than 273° K. In comparison with the 28 January 1986 cross-shelf air temperature differences, the values observed for this mission (6.4° K) were comparable to those measured earlier in this general vicinity by the NCAR Electra (5.4° K, Mission R-6). The resulting cross-shelf air temperature gradient was $0.0538° \text{ K} \cdot \text{km}^{-1}$, which is greater than the value observed by the NCAR Electra for this general area on 28 January 1986. Contributing to this difference was the highest observed low-level air temperature gradient during all the aircraft operations which was found during this mission between Stations B and C ($0.0706° \text{ K} \cdot \text{km}^{-1}$).

The mean specific humidity profiles for NCAR King Air Missions R-15 and R-16 were also moister than those observed by the NCAR Electra on this date. Each of these profiles also corroborated the inversion level determined in the respective potential temperature profile and also displayed the characteristics of a well-mixed convective boundary layer. The observed low-level specific humidity values ranged from $3.36 \text{ g} \cdot \text{kg}^{-1}$ over the mid-shelf (Station A) to $4.58 \text{ g} \cdot \text{kg}^{-1}$ in the vicinity of the Gulf Stream Front (Station B) where SST gradients are the largest, to their maximum value of $4.96 \text{ g} \cdot \text{kg}^{-1}$ over the core of the Gulf Stream (Station C). The cross-shelf moisture gradient (Station A to C) was $0.0134 \text{ g} \cdot \text{kg}^{-1} \cdot \text{km}^{-1}$ which was slightly larger than the values computed for the other three aircraft missions. However, the moisture gradient computed across the Gulf Stream Front was $0.0238 \text{ g} \cdot \text{kg}^{-1} \cdot \text{km}^{-1}$, which is almost twice the overall cross-shelf gradient. Thus, very strong air mass modification is occurring across this relatively narrow (~50 km) oceanic frontal zone.

4.2. Turbulent structure

Figure 9 shows the normalized temperature and humidity flux profiles for all the NCAR Electra and King Air missions flown on 28 January and 12 February 1986. The normalized sensible heat flux profiles (using potential temperature) below z/h are essentially linear and can be described by:

$$\frac{(\overline{w'\theta'})}{(\overline{w'\theta'})_0} = 1 - 1.28\left(\frac{z}{h}\right), \tag{1}$$

while the sensible heat flux profiles (using virtual potential temperature) are best fit as:

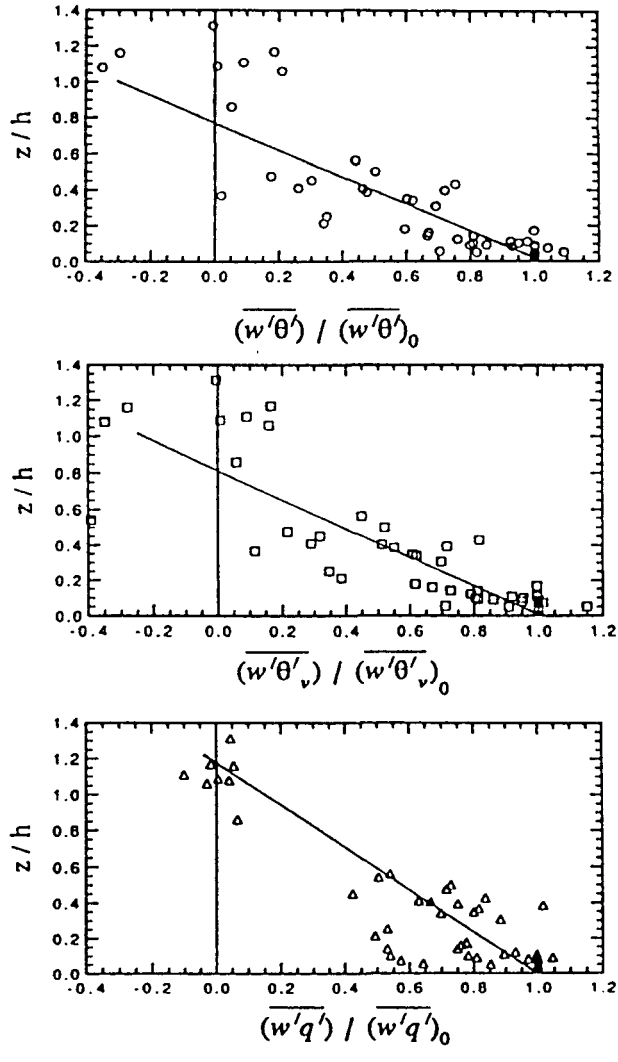

Fig. 9. Normalized heat and water vapor flux profile relationships for the combined NCAR Electra and King Air Missions on 28 January 1986 and 12 February 1986. All data points collected are shown. However, the best fit lines are for data below $0.9z/h$.

$$\frac{(\overline{w'\theta'_v})}{(\overline{w'\theta'_v})_0} = 1 - 1.25\left(\frac{z}{h}\right). \tag{2}$$

The cloud-top crosswind flux data have been omitted in order to compare these results with other investigations of MABL structure, where only data within the MABL were analyzed (Wyngaard *et al.*, 1978; Chou *et al.*, 1986; Chou and Zimmerman, 1989; Chou and Ferguson, 1991). The associated specific humidity flux profile is also nearly linear and can be best described by

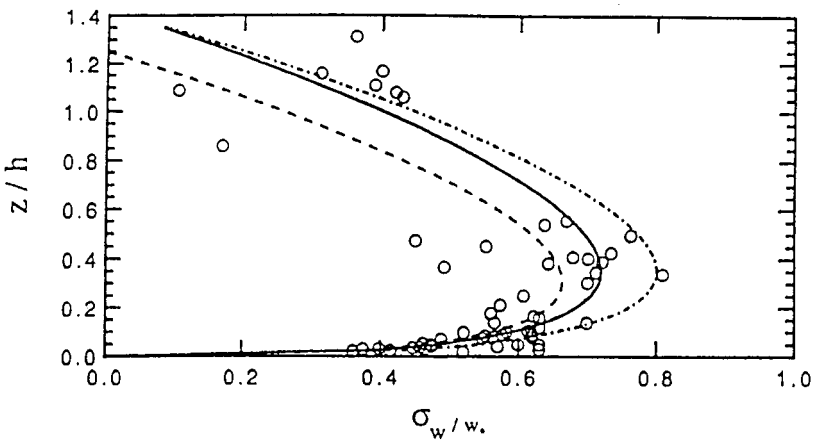

Fig. 10. Normalized vertical velocity component standard deviations (σ_w) relationship for the combined NCAR Electra and King Air missions on 28 January 1986 and 12 February 1986. The dashed line represents the results of Lenschow *et al.* (1980) for the AMTEX data and the dot-dash line is the relationship observed for the MASEX data (Chou *et al.*, 1986). The solid curve is the best fit polynomial for the current study and is given by Equation (7) in the text.

$$\frac{(\overline{w'q'})}{(\overline{w'q'})_0} = 1 - 0.84\left(\frac{z}{h}\right). \tag{3}$$

When compared to the MASEX results (Chou et al., 1986), reasonably good agreement is found with the temperature flux profile data, but no relationship for the MASEX humidity data was found due to a large amount of scatter in this data set. Chou *et al.* (1986) attributed this scatter to the absence of adequate mixing of moisture within the MASEX MABL. However, they were able to derive a suitable relationship for the temperature flux data, below $0.9z/h$. Additionally, the AMTEX results of Wyngaard *et al.* (1978) and the 28 January 1986 results of Chou and Ferguson (1991) also correlate well with the current observations.

The vertical velocity component standard deviations (σ_w) for 28 January and 12 February 1986 also show relatively good agreement with earlier observational studies. The best-fit polynomial is provided for these data by

$$\frac{\sigma_w}{w_*} = 1.35\left(\frac{z}{h}\right)^{0.33}\left[1 - 0.7\left(\frac{z}{h}\right)\right], \tag{4}$$

which is similar in shape to the AMTEX results of Lenschow *et al.* (1980) and the MASEX observations of Chou *et al.* (1986). The value of 1.35 is slightly larger than the calculated AMTEX value, but is less than the MASEX value, indicating a closer correlation between these results and the AMTEX observations. Figure 10 shows the normalized vertical velocity component standard deviations (σ_w) along with the curves for the AMTEX data, MASEX data and Equation (4). The

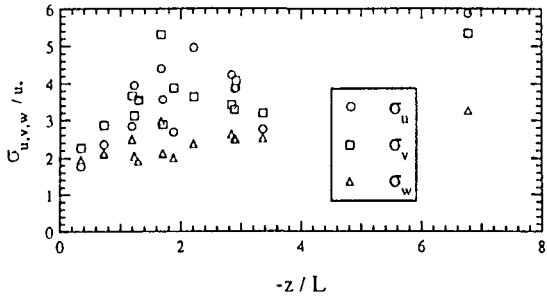

Fig. 11. Normalized surface layer standard deviations of the velocity components (σ_u, σ_v, σ_w) for the combined aircraft missions on 28 January 1986 and 12 February 1986.

dashed line represents the AMTEX results of Lenschow *et al.* (1980), while the dot-dash line is the equation generated from the MASEX data (Chou *et al.*, 1986). The solid line represents Equation (4) and clearly provides the best fit to the combined 28 Januaryand 12 February 1986 data sets. This equation yields a maximum value near $0.4z/h$, which is in good agreement with other observational and modelling studies. Thus, the different observational studies compare favorably with the current investigation, further indicating the validity of the similarity relations under the higly convective conditions observed during a cold air outbreak, downwind (~25 km) of sharp SST discontinuities.

In investigating surface-layer turbulence for the combined 28 January and 12 February 1986 aircraft missions, only data collected at the lowest flight level for each crosswind research station were analyzed. Figure 11 shows the normalized standard deviations of the velocity components (σ_u, σ_v, σ_w) at each of these levels plotted versus $-z/L$. Previous research has shown that the horizontal velocity components (σ_u, σ_v) of turbulence within the surface layer generally do not follow either Monin–Obukhov or local free convection scaling (Arya, 1988). This appears to be the case in Figure 12, where local advective effects tend to cause the horizontal velocity components to adhere better to mixed-layer scaling (e.g., for $-h/L \gg 1$, $\sigma_{u,v} \sim w_*$). This tendency implies that σ_w/w_* is proportional to $(-h/L)^{1/3}$. Figure 12 shows the horizontal velocity components plotted versus $-h/L$; the data show reasonably good agreement with the earlier results of Panofsky *et al.* (1977), where the following relationships have been prescribed:

$$\frac{\sigma_{u,v}}{u_*} = \left[4.0 + 0.6\left(\frac{-h}{L}\right)^{2/3}\right]^{1/2} \tag{5}$$

$$\frac{\sigma_{u,v}}{u_*} = \left[12.0 - 0.5\left(\frac{h}{L}\right)\right]^{1/3}. \tag{6}$$

These equations are represented by the solid and dashed lines, respectively, in Figure 12. Equation (5) is similar in form to that postulated by Wyngaard and

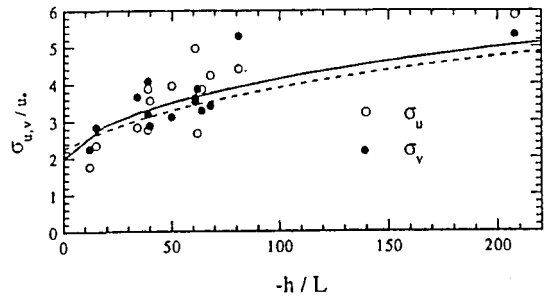

Fig. 12. Normalized surface-layer standard deviations of the horizontal velocity components (σ_u, σ_v) for the combined aircraft missions on 28 January 1986 and 12 February 1986. The lines represent the relationships of Panofsky *et al.* (1977) which are given in Equations (5) and (6).

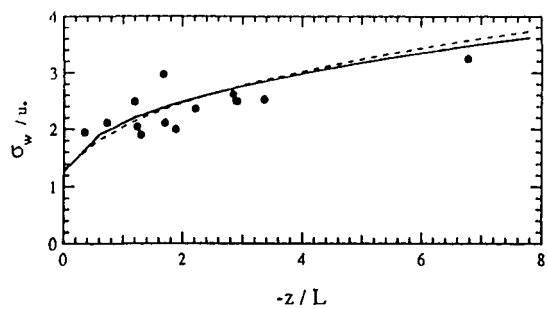

Fig. 13. Normalized surface-layer standard deviations of the vertical velocity component (w_*) for the combined NCAR Electra and King Air missions on 28 January 1986 and 12 February 1986. The lines represents the relationships of Panofsky *et al.* 1977) which are given in Equations (7) and (8).

Coté (1974), while Equation (6) provides good agreement with the data but in a less complex format. However, the difference in magnitude between the horizontal and vertical velocity components is much less in the current investigation than in the earlier marine surface layer results from BOMEX, described by Leavitt and Paulson (1975). This difference can be attributed to stronger convective and baroclinic (e.g., advection) conditions on 28 January and 12 February 1986.

On the other hand, previous observational studies have shown that normalized surface-layer standard deviations of the vertical velocity component (σ_w) generally show reasonable agreement with local free convection scaling (e.g., $\varphi_w/u_* \sim (-z/L)^{1/3}$) for large values of $-z/L$ (Arya, 1988). Figure 13 presents the combined normalized standard deviations of the vertical velocity component for the combined aircraft missions of 28 January and 12 February 1986 plotted versus $-z/L$. These data also show good agreement with the relationships derived by Panofsky *et al.* (1977) which are given as follows

$$\frac{\sigma_w}{u_*} = \left[1.6 + 2.9\left(\frac{-z}{L}\right)^{2/3}\right]^{1/2} \tag{7}$$

$$\frac{\sigma_w}{u_*} = 1.3\left[1.0 - 3.0\left(\frac{z}{L}\right)\right]^{1/3} \tag{8}$$

Equation (7) is represented by the solid line in Figure 13, while the dashed line is described by Equation (8). Thus, the surface-layer standard deviations of the velocity components compare favorably with the earlier observations of Panofsky *et al.* (1977). Again, Equation (7) is similar in form to that postulated by Wyngaard and Coté (1974) and Businger (1959), while Equation (8) provides a similar fit to the observations, but in a simpler format.

The extreme air-SST values observed for the 28 January 1986 aircraft missions resulted in a tremendous flux of energy from the ocean surface layer into the MABL. The maximum observed total (sensible + latent) heat fluxes (1045 and 983 $W \cdot m^{-2}$, respectively) were recorded over the core of the Gulf Stream for both aircraft missions, while stations both seaward and landward had substantially lower values. For the Electra mission (R-6), values ranged from 516 $W\ m^{-2}$ along the inner shelf to 988 $W \cdot m^{-2}$ at the Western Wall of the Stream. On the eastern edge of the Stream, total heat flux observations reduced to 687 $W \cdot m^{-2}$. For the NCAR King Air mission (R-8), Stations A and C yielded values of 580 and 683 $W \cdot m^{-2}$, respectively. As was discussed in Section 4.1, Stations A and C were sampled approximately two hours apart over essentially the same geographic area. Thus, the temporal rate of change in total heat flux along the shelf offshore of Cape Hatteras was approximately 50 $W \cdot m^{-2} \cdot h^{-1}$.

The NCAR Electra encountered a mean SST gradient from Stations A to C of 0.068 $°C \cdot km^{-1}$. This value was higher than the gradient observed by Chou *et al.* (1986) during the MASEX study (0.057 $°C \cdot km^{-1}$). Due to the pre-flight failure of the downward-looking radiometer, no SST data were available for the NCAR King Air mission. However, using the AVHRR satellite images, the SST at Station A was estimated to be ~18 °C, while the Gulf Stream core temperature was estimated to be near 23 °C. Thus, the estimated mean SST gradient in this region was computed to be 0.077 $°C \cdot km^{-1}$, which was considerably stronger than either the gradient observed by the NCAR Electra or those reported during MASEX.

As was expected for the moderate cold air outbreak conditions on 12 February 1986, the calculated sensible and latent heat fluxes were considerably lower than those observed during the 28 January 1986 event. The maximum observed total heat fluxes were 811 and 668 $W\ m^{-2}$, respectively for the NCAR Electra and King Air aircraft. Again these observations were recorded over the core of the Gulf Stream and were approximately 250 to 300 $W\ m^{-2}$ less than their respective 28 January 1986 observed values. However, the near-surface heat fluxes showed the same patterns observed in the earlier flights, increasing between the shelf and the Stream before decreasing towards the Sargasso Sea region. In general, the latent

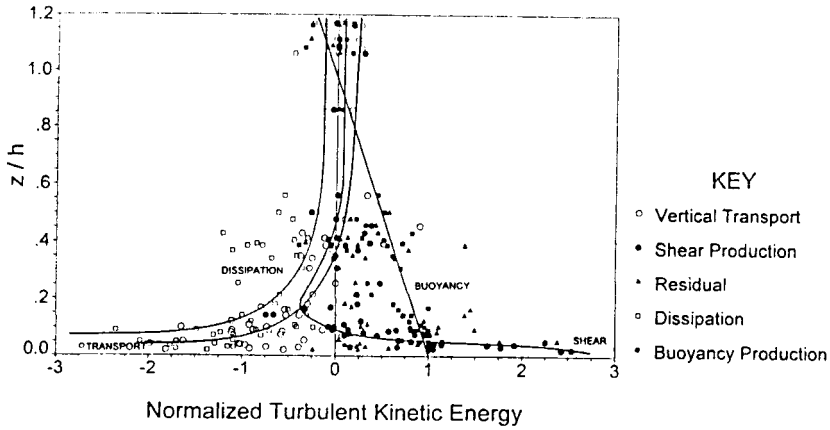

Fig. 14. Normalized Turbulent Kinetic Energy (TKE) budget for the four aircraft missions flown by the NCAR Electra and King Air aircraft on 28 January and 12 February 1986. Each data point has been normalized by the low-level buoyancy parameter for its respective location.

heat flux values were twice the sensible heat flux estimates, except for the 28 January 1986 NCAR King Air mission (R-8) where the individual components of the total heat flux budget were observed to be approximately equal in magnitude.

The computed SST gradients between the inner shelf and the core of the Stream varied significantly for these two aircraft missions. The NCAR Electra (R-14) observed a SST gradient of $0.144\,^{\circ}\mathrm{C}\cdot\mathrm{km}^{-1}$, while the King Air (R-15/16) observed a gradient of $0.042\,^{\circ}\mathrm{C}\cdot\mathrm{km}^{-1}$. The former value is considerably higher than the earlier observations discussed above, while the latter is considerably lower than the gradients observed on any of the previous aircraft missions or the MASEX data. The high SST-gradient observed by the NCAR Electra is caused by the trajectory of the Stream being in close proximity to Diamond Shoals and the shallow, cold inner shelf water. For the 28 January 1986 CAO, the Stream was in a deflected pattern farther offshore from the Hatteras Corner, resulting in lower SST gradients.

In summarizing the turbulent structure of the MABL offshore of North Carolina, the normalized TKE budget for all four research missions flown during 28 January and 12 February 1986 is given in Figure 14. Each station has been normalized by the low-level buoyancy flux to make the budget non-dimensional. As would be expected under such a convective regime, buoyancy production provided the major generation of turbulent energy between $0.1 \leqslant z/h \leqslant 0.8$. Above this level, vertical transport became the dominant source term in the budget. The vertical transport of TKE is negative below $0.4z/h$, indicating a net loss of energy from the lower MABL to the upper regions of the boundary layer.

The production side of TKE budget below $0.1z/h$ is dominated by shear production, as observed in the low-level acceleration of the wind field towards the Gulf Stream Front. The observed negative minimum in the shear production curve has

been attributed to the presence of the low-level jet feature, which was not observed for the 12 February 1986 research stations due to the more northerly wind conditions on this date. However, when aggregating all the research missions in a single figure, the strength of this feature persists and is thus included. Dissipation is the primary destructive agent in the budget prior to entrainment effects causing the negative buoyancy term (e.g., entrainment) to become the dominant term on the negative side of the budget. The entrainment effects were visibile during the cloud top runs, as penetrative cumulus cells pushed upward through the mixed layer into the free atmosphere. In general, there was good general agreement between the TKE budgets of the individual research missions.

5. Summary

The evolution of the wintertime Marine Atmospheric Boundary Layer (MABL) along the southeastern United States coast is a very complex phenomenon, which is driven by the energy exchange processes between the ocean-atmosphere system. The ocean-atmosphere exchanges are maximized in the winter months by synoptic events known as cold air outbreaks (CAOs). The air-SST gradient can reach $-25\,^{\circ}C$ during an intense cold air outbreak, causing extremely large sensible and latent heat fluxes to be observed over these regions.

During the Genesis of Atlantic Lows Experiment (GALE), evolution and response of the MABL were studied during two CAOs offshore of North Carolina in close proximity to the Gulf Stream system. These two case studies focused on the strong, intense CAO of 28 January 1986 and the moderate CAO of 12 February 1986. The investigations involved the use of a variety of aircraft, surface, upper air and satellite measurements to document the mean and turbulent structure of the MABL.

The ocean-atmosphere energy exchanges during the CAO caused the oncoming air mass to warm and moisten as it moved across the warmer coastal waters offshore of North Carolina. The primary observed mechanism for these exchanges was the transfer of sensible and latent heat between the ocean and the overlying atmosphere. During the intense CAO of 28 January 1986, the total heat flux measured over the core of the Gulf Stream (49 m ASL) was 1045 and 983 $W\,m^{-2}$ offshore of Wilmington and Cape Hatteras, North Carolina, respectively. The heat flux values measured both landward and seaward of this region were found to be less than these maxima. Additionally, the values observed during the 28 January 1986 CAO were considerably larger than those measured during earlier projects designed to investigate these events: MASEX; AMTEX '74; Winter MONEX; and, Pre-GALE. However, there was one CAO event during AMTEX '75 which produced comparable heat flux estimates in the region surrounding the Kuroshio Current. Examining the milder CAO studied during this investigation (12 February 1986), the maximum observed heat fluxes (668 $W\,m^{-2}$ and

811 W m^{-2}) were once again measured near the core of the Gulf Stream, offshore of Cape Lookout (35 m ASL) and Cape Hatteras (47 m ASL), North Carolina, respectively. These results were much more compatible with the flux estimates obtained during the earlier observational studies. Once again, the heat flux estimates decreased both landward and seaward of the observed maxima over the core of the Stream on 12 February 1986.

In response to these large fluxes of energy into the lower MABL, boundary-layer height (h) increased steadily in the offshore direction during all four aircraft missions. Accompanying this increase in height was a concomitant decrease in cloud-base altitude, which effectively increased the depth of the cloud layer contained within the MABL. The deepening of the cloud layer in the downwind direction resulted in the majority of the MABLs over the Gulf Stream and the Sargasso Sea areas being contained within the clouds. This scenario was most obvious in the 28 January 1986 NCAR Electra mission (R-6), where cloud base altitude decreased continuously from the shelf out to the Sargasso Sea area, while boundary-layer height (e.g., cloud-top altitude) grew to approximately 2300 m. However, this phenomenon was observed to some extent in the three remaining aircraft missions, but the decline in cloud base altitude and the associated increases in the cloud-top altitude were not as dramatic.

The MABL adjusted almost instantaneously to downwind changes in the underlying SST conditions, as evidenced by the normalized flux profiles, which showed general agreement at the different crosswind flight locations flown for each aircraft mission. This result is indicative of similar processes contributing to the air mass modification over each of the four oceanic zones sampled: inner shelf; mid-shelf (Gulf Stream Front); Gulf Stream core; and Sargasso Sea. Heat flux profiles obtained from both the potential temperature (θ) and the virtual potential temperature (θ_v) flux profiles showed the characteristics of a well-mixed, convective boundary layer. The near-surface maximum at each crosswind research location was subsequently followed by a near-linear decrease in magnitude with increasing height within the MABL. The turbulent sensible heat flux profiles for each aircraft mission showed the effects of entrainment near the inversion level, where negative buoyancy values were observed above $0.8z/h$ for the missions having crosswind levels at these altitudes. The specific humidity flux profiles also displayed the characteristic well-mixed, convective boundary-layer shape, having both the near-surface maxima and the near-linear decrease in magnitude with increasing height.

The two horizontal velocity components (u, v) were observed to contribute approximately equally to the turbulence during all four aircraft missions. The general agreement between each of the individual missions was good and the level of turbulent energy was observed to decrease with increasing height in the MABL. Evidence of high-level shear at the top of the boundary layer was also observed during the missions over the wider southern North Carolina shelf (R-6 and R-15, R-16). The vertical velocity component (w) also exhibited the characteristic well-

mixed, convective boundary-layer profile where a mid-level ($\sim 0.4z/h$) maximum is observed and values decrease both above and below this region within the MABL.

The Turbulent Kinetic Energy (TKE) budget constructed for the two CAOs showed general agreement, but with two major differences. First, the 28 January 1986 results showed a strong low-level (~ 110 m) jet at all crosswind research locations, which generated a negative maximum in the shear production curves for these two aircraft missions (R-6 and R-8). This result has been attributed to the strong baroclinic conditions on this date, which caused the near-surface winds to accelerate towards the Gulf Stream. The absence of this jet feature, the more northerly mean synoptic wind field and in general the milder atmospheric conditions on 12 February 1986 account for the absence of the low-level maxima in the shear production curves for 12 February 1986. Secondly, the entrainment effects on 12 February 1986 were observed to be stronger than in the earlier investigation, which coupled with weaker SST gradients generated lower MABL heights for this CAO. Except for NCAR King Air Mission R-8, the MABL was dominated by shear production below $0.1z/h$. Mission R-8, which was conducted offshore of Cape Hatteras in a region of strong surface thermal contrast, was dominated by buoyancy production throughout the lower MABL. The negative side of all four budgets was dominated by dissipation of turbulent energy at the mid- and lower levels and by entrainment effects near the inversion layer. Additionally, vertical transport of turbulent energy was also a loss term in these budgets below approximately $0.5z/h$. Overall, the budgets showed general agreement with each other and with the previous observational studies.

In general the MABL investigated during 28 January 1986 was considerably more convective than the environment observed on 12 February 1986. Additionally, the earlier investigations of CAOs (e.g., AMTEX, MASEX, Winter MONEX and Pre-GALE) also were less energetic than the 28 January 1986 CAO, and were more closely related to the conditions observed during the milder 12 February 1986 investigation. Nonetheless, the comparison between these earlier observational data sets and the current results has shown in general reasonably good agreement.

Acknowledgements

This work was partially supported by the Division of Atmospheric Sciences, National Science Foundation (NSF) under grant ATM-9212636 and Science Applications International Corporation's (SAIC) Maritime Technology Group (Marine Science and Engineering Division) and Integrated Technology Applications Group (Technology Assessment Division).

References

Arya, S. P. S.: 1988, *Introduction to Micrometeorology*, Volume 42, International Geophysics Series, Academic Press, Incorporated, London, 307 p.

Bane, J. M. and Osgood, K. E.: 1989, 'Wintertime Air-Sea Interaction Processes Across the Gulf Stream', *J. Geophys. Res.* **94**(C8), 10755–10772.

Brümmer, B., Rump, B., and Kruspe, G.: 1992, 'A Cold Air Outbreak Near Spitsbergen in Springtime – Boundary Layer Modification and Cloud Development', *Boundary-Layer Meteorol.* **61**, 13–46.

Businger, J. A.: 1959, 'A Generalization of the Mixing-Length Concept', *J. Meteorol.* **16**, 516–523.

Chou, S.-H. and Ferguson, M. P.: 1991, 'Heat Fluxes and Roll Circulations over the Western Gulf Stream during an Intense Cold Air Outbreak', *Boundary-Layer Meteorol.* **55**, 255–281.

Chou, S.-H. and Zimmerman, J.: 1989, 'Bivariate Conditional Sampling of Buoyancy Flux during an Intense Cold Air Outbreak', *Boundary-Layer Meteorol.* **46**, 93–112.

Chou, S.-H., Atlas, D. and Yeh, E.-N.: 1986, 'Turbulence in a Convective Marine Atmospheric Boundary Layer', *J. Atmos. Sci.* **43**(6), 547–564.

Chou, S.-H. and Atlas, D.: 1982, 'Satellite Estimates of Ocean-Air Heat Fluxes during Cold-Air Outbreaks', Mon. Wea. Rev. **110**, 1434–1450.

Dirks, R. A., Kuettner, J. P. and Moore, J. A.: 1988, 'Genesis of Atlantic Lows Experiment (GALE): An Overview', *Bull. Amer. Meteorol. Soc.* **69**(2), 148–160.

Fernandez-Partegas, J. and Mooers, C. N. K.: 1975, 'A Subsynoptic Study of Winter Cold Fronts in Florida', *Mon. Wea. Rev.* **103**, 742–744.

Grossman, R. L.: 1988, 'Boundary Layer Warming by Condensation: Air-Sea Interaction during an Extreme Cold Air Outbreak from the Eastern Coast of the United States', *Preprint, Seventh Conference on Ocean-Atmosphere Interaction*, Amer. Meteorol. Soc., January 31–February 5, 1988, Anaheim, California.

Grossman, R. L. and Betts, A. K.: 1990, 'Air-Sea Interaction during an Extreme Cold Air Outbreak from the Eastern United States', *Mon. Wea. Rev.* **118**(2), 324–242.

Huh, O. K., Rouse, L. J. and Walker, N. D.: 1984, 'Cold-Air Outbreaks over the Northwest Florida Continental Shelf: Heat Flux Processes and Hydrographic Changes', *J. Geophys. Res.* **89**(C1), 717–726.

Johnson, R. H. and Zimmerman, J. R.: 1986, 'Modification of the Boundary Layer over the South China Sea during a Winter MONEX Cold Surge Event', *Mon. Wea. Rev.* **114**(11), 2004–2015.

Kondo, J.: 1976, 'Heat Balance of the East China Sea during the Air Mass Transformation Experiment', *J. Meteorol. Soc. Jpn.* **54**, 382–398.

Konrad, T. G. and Colucci, S. J.: 1989, 'An Examination of Extreme Cold Air Outbreaks over Eastern North America', *Mon. Wea. Rev.* **117**, 2687–2700.

Leavitt, E. and Paulson, C. A.: 1975, 'Statistics of Surface Layer Turbulence over the Tropical Ocean', *J. Phys. Ocean.* **5**, 143–156.

Lenschow, D. H. and Agee, E. M.: 1976, Preliminary Results from the Air-Mass Transformation Experiment (AMTEX)', *Bull. Amer. Meteorol. Soc.* **57**, 1346–1355.

Lenschow, D. H., Wyngaard, J. C. and Pennel, W. T.: 1980, 'Mean and Second Moment Budgets in a Baroclinic, Convective Boundary Layer', *J. Atmos. Sci.* **37**(6), 1313–1326.

Mercer, T. J. and Kreitzberg, C. W.: 1986, *GALE Field Program Summary*, GALE Data Center (GDC), Drexel University, Philadelphia, Pa., 447 p.

Panofsky, H. A., Tennekes, H., Lenschow, D. H. and Wyngaard, J. C.: 1977, 'The Characteristics of Turbulent Velocity Components in the Surface Layer under Convective Conditions', *Boundary-Layer Meteorol.* **11**, 355–361.

Raman, S. and Riordan, A. J.: 1988, 'The Genesis of Atlantic Lows Experiment: The Planetary Boundary Layer Subprogram', *Bull. Amer. Meteorol. Soc.* **69**(2), 161–172.

SethuRaman, S., Riordan, A. J., Holt, T., Stunder, M. and Hinman, J.: 1986, 'Observations of the Marine Boundary Layer Thermal Structure over the Gulf Stream during a Cold-Air Outbreak', *J. Clim. Appl. Meteorol.* **25**(1), 14–21.

Uccellini, L. W., Brill, K. F., Petersen, R. A., Keyser, D., Aune, R., Kocin, P. J. and des Jardins M.: 1986, 'A Report on the Upper Level Wind Conditions Preceding and during the Shuttle Challenger (STS 51L) Explosion', *Bull. Amer. Meteorol. Soc.* **67**(10), 1248–1265.

Wayland, R. J.: 1991, *Mean and Turbulent Structure of the Marine Atmospheric Boundary Layer during Cold Air Outbreaks of Different Intensities: Observational and Modeling Analyses (GALE 86)*, Ph.D. Dissertation, North Carolina State University, Raleigh, North Carolina, 388 p.

Wayland, R. J. and Raman S.: 1989, 'Mean and Turbulent Structure of a Baroclinic Marine Boundary Layer during the 28 January 1986 Cold Air Outbreak (GALE 86)', *Boundary-Layer Meteorol.* **8**, 227–254.

Wyngaard, J. C., Pennell, W. T., Lenschow, D. H. and LeMone M. A.: 1978, 'The Temperature-Humidity Covariance Budget in the Convective Boundary Layer', *J. Atmos. Sci.* **35**, 47–58.

Wyngaard, J. C. and Coté, O. R.: 1974, 'The Evolution of a Convective Planetary Boundary Layer – A Higher-Order Closure Model Study', *Boundary-Layer Meteorol.* **7**, 289–308.